ACS Sustainable Chemistry & Engineering

Research Article

pubs.acs.org/journal/ascecg

Biobased Thermosetting Epoxy Foams: Mechanical and Thermal Characterization

Facundo I. Altuna,* Roxana A. Ruseckaite, and Pablo M. Stefani

Institute of Materials Science and Technology (INTEMA), National Research Council-National University of Mar del Plata (CONICET-UNMdP), Juan B. Justo 4302, Mar del Plata, Argentina

Supporting Information

ABSTRACT: Thermosetting epoxy foams were synthesized by replacing the commercial synthetic epoxy resin by a biogenic epoxidized vegetable oil. Foam formulations were developed avoiding the use of amine hardeners, organic volatile compounds (OVCs), and ozone depleting or flammable foaming gases. The produced biobased foams were evaluated in terms of mechanical and thermal properties. It was found that the glass transition temperature (Tg) is somewhat lower than that corresponding to synthetic epoxy foams, but mechanical properties are similar when comparing foams of the same density. Moreover, the possibility of obtaining foams in a wide range of densities (160−550 kg/m^3) makes these systems a sound alternative to commercial available formulations.

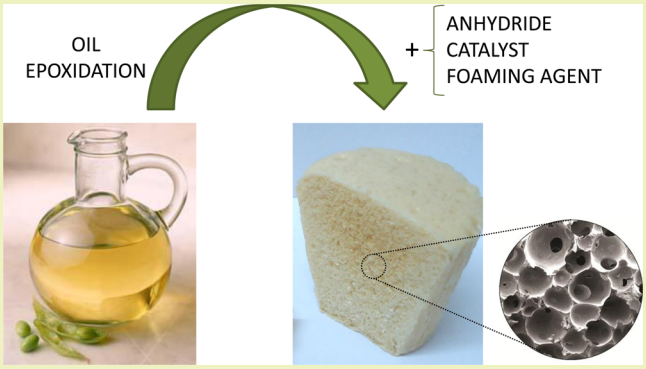

KEYWORDS: *Green chemistry, Vegetable oil, Thermosetting polymer, Epoxy, Anhydride hardener, Rigid foams*

INTRODUCTION

Thermosetting epoxy foams are lightweight materials extensively used in many industrial areas, such as aircraft, automotive, building, or electronics, owing to their low density combined with a unique set of properties, such as high mechanic strength, good thermal and chemical stability, excellent dielectric properties, and adhesion to a variety of substrates.[1,2] Unfortunately, most of the monomers available today to prepare epoxy resins are derived from petroleum sources, accounting for about 7% of worldwide oil and gas consumption.[3] The rising cost of oil as well as the awareness over limited fossil fuel reserves has renewed the interest in renewable sources of polymer feedstock to substitute at least a fraction of their petrochemical-sourced equivalent.[4,5] Although the recent developments using biomass-derived materials have achieved great progress, the small share (<5%) of renewable polymers in the commercial market is largely due to their poor cost/performance competitiveness in many market applications.[6] Facing this technical challenge, academic and industrial laboratories are intensively working to find efficient ways to transform such bio-feedstock into highly functional raw materials.[7,8]

Naturally occurring plant oils are a valuable and worldwide accessible bioresource that can provide alternatives for the chemical industry. However, vegetable oils must meet several requirements in order to compete with synthetic monomers or prepolymers; therefore their functionalization to tailor new structures has been a matter of intensive study.[9−12] Epoxidation of double bonds to obtain epoxidized vegetable oils (EVOs)[7] is one of the main strategies to convert vegetable oils into numerous valuable products, such as precursors in formulations of thermosetting polymers.[13−17]

Reports on the application of EVOs in the synthesis of epoxy foams are, nevertheless, scarce. Bonnaillie and Wool[18] reported the synthesis of thermosetting foams with acceptable mechanical properties from acrylated epoxidized soybean oil (AESO) using CO_2 dissolved at high pressure as a foaming agent. Yadav et al.[19] synthesized epoxy foams containing 12.5 to 25 wt % of biogenic component, and Dogan and Küsefoğlu[20] used malonic acid (MA) as a simultaneous foaming and cross-linking agent for epoxidized soybean oil (ESO). However, in both cases the mechanical properties were poor. More recently, Lau et al.[21] developed foams from a partially biobased commercial epoxy-amine system, showing excellent mechanical properties. Among the aforementioned studies, only a few of them[18,21] were successful in producing foams with mechanical properties comparable to those of commercially available systems. Nonetheless, these methods lead to the production of foams within a limited range of densities, without a straightforward strategy to control the final density.

In a previous work, we demonstrated the feasibility of synthesizing syntactic foams from epoxy copolymers with high ESO content as a biogenic component, with comparable compressive and flexural properties to those obtained from neat

Received: February 18, 2015
Revised: May 6, 2015
Published: May 22, 2015

DOI: 10.1021/acssuschemeng.5b00114
ACS Sustainable Chem. Eng. 2015, 3, 1406−1411

diglycidyl ether of bisphenol A (DGEBA).[22] In the present study, we report the preparation of thermosetting epoxy foams using high contents of ESO (not less than 55 wt %) as a biogenic component. Sodium bicarbonate was selected as a low cost, nontoxic, and safe thermally latent foaming agent, and a low toxicity carboxylic acid anhydride (methyltetrahydrophtalic anhydride) was chosen as curing agent. The physical, dynamic mechanical, and compressive properties were assessed, and the effect of the foaming agent content on them was discussed. The foams were compared in terms of their performance with a synthetic epoxy foam and with other biobased foamed systems.

EXPERIMENTAL SECTION

Materials. Epoxidized soybean oil (ESO; epoxy equivalent weight: 241 g/eq) was kindly supplied by Unipox SA (Buenos Aires, Argentina). ESO was dehydrated under vacuum before use. Methyl tetrahydrophtalic anhydride (MTHPA; anhydride equivalent weight: 166 g/eq), and 1-methyl imidazole (1MI) were purchased from Huntsman (Buenos Aires, Argentina) and used as received. A mixture of stearic and palmitic acid (67:33 wt %) was kindly provided by Materia Oleochemicals (Mar del Plata, Argentina) and used as a surfactant. Sodium bicarbonate ($NaHCO_3$) was selected as an innocuous thermally latent foaming agent (FA).

Preparation. ESO foams were prepared by the reaction of ESO with the stoichiometric amount of MTHPA and 1MI as an initiator following the protocol described in our previous works,[15,22−24] with $NaHCO_3$ as a foaming agent at varying proportions. Briefly, 23.2 g of ESO, 16 g of MTHPA, 0.48 g of 1MI, and 0.32 g of surfactant were mixed together in an aluminum disposable cup (of about 4−6 cm in diameter by about 6 cm height) to produce 40 g of reactive mixture. Subsequently, the desired amount of FA (0.6 to 2.8 g, corresponding to FA contents from 1.5 to 7 wt %, respectively) was added, and manual mixing was carried out gently, preventing the occlusion of air bubbles. The total biogenic content (wt % of ESO and surfactant) of each foam is within the range of 58.2% to 55%, these values corresponding to FA contents of 1% and 7%, respectively. Free foaming was performed by heating the mixture at 140 °C in a convection oven (Yamato DKN400; San Francisco, USA).

The temperature−time profile during the simultaneous foaming and curing processes was measured every 15−20 s, using a thermocouple immersed in the reaction mixture. Cream time (t_{cr}) was estimated at the time at which the reactive mixture changed from a transparent or translucent appearance to a pale yellow opaque one (due to the presence of bubbles), and the foaming process started. The approximate value of gelation time (t_{GEL}) was measured by gently pulling upon the thin wires of the thermocouple and quoting the time at which the wire become entrapped in the gel.[25] The conversion vs time curves were predicted from experimental temperature−time profile by using the Kamal−Sourour kinetic equation,[26] together with the kinetic parameters obtained for the nonfoamed systems[27] (a more detailed explanation is available in the Supporting Information). Figure 1 shows thermosetting foams based on the ESO/MTHPA/1MI polymeric matrix.

Methods. The apparent density (ρ^*) was calculated by determining experimentally the weight and volume of prism-shaped foam samples (10 mm height × 20 mm × 20 mm square section). Specimens were taken from the bottom, medium, and top regions of the foams to report average apparent density values for each formulation. Weight was registered with an Ohaus Adventurer AR2140 analytical balance (New Jersey, USA) with a precision of 0.1 mg, and dimensions were measured with a Mitutoyo caliper (Kawasaki, Japan) with a precision of 0.01 mm. Reported results were the average of at least five measurements.

Porosity (e) was calculated according to eq 1:

$$e = 1 - (\rho^*/\rho_s) \quad (1)$$

where ρ^* is the foam apparent density and ρ_s is the polymeric matrix density taken from our previous work (ρ_s = 1115 kg/m^3).[22]

Figure 1. Thermosetting foams based on ESO/MTHPA/1MI polymeric matrix.

The morphology and internal structure of the produced foams was investigated by scanning electron microscopy (SEM). A Jeol JSM-6460LV (Tokyo, Japan) SEM was used at an accelerating voltage of 10 kV to obtain images of horizontal and vertical planes of the foams. Samples were taken from the middle region, and before observation surfaces were sputter-coated with a thin layer of gold to prevent charging under the electron beam. SEM images were used to calculate the average diameter (Dc) and average number by surface area unit (n) of the foam cells with a representative sample population of about 50 cells.

Compressive tests were conducted according to the ASTM D-1621 standard, at room temperature (22 °C) using an Instron 4467 universal testing machine (Buckinghamshire, England) and at a crosshead speed of 1.3 mm/min. Square-section (20 × 20 mm^2) specimens with a height of 10 mm, in both the growth direction and transversal direction, were used. Compressive specimens were extracted from the center of the foams, and regions close to the external surface were discarded due to irregularities in the morphology induced by the mold walls. Teflon sheets were placed between the specimen and each plate during tests to minimize friction. The compressive apparent modulus (E^*) was determined from the initial slope of the compressive stress−strain curve. The compressive strength (σ_c) defined as the plateau in stress subsequent to the initial linear loading region was calculated at a strain of 10%. Reported results were the average of at least three measurements.

Dynamic mechanical analysis was performed on rectangular-shaped specimens (dimensions: 3 × 8 × 30 mm^3) using an Anton Paar Physica MCR 301 rheometer in torsion mode at a fixed frequency of 1 Hz, at an oscillation amplitude of 0.1%, and with a distance between clamps of 21 mm. Storage shear modulus (G') and damping factor ($\tan\delta$) were recorded as a function of the temperature, from −60 to 200 °C, at a heating rate of 2 °C/min. For comparison purposes, a nonfoamed sample was tested under the same conditions. These tests were run in duplicate.

One-way analysis of variance (ANOVA), together with the Tukey test for pair comparison were employed to examine differences between groups, with a significance of the difference set at (α) < 0.05.

RESULTS AND DISCUSSION

Curing and Foaming Process. Conditions to achieve simultaneous curing and foaming were defined from previous works[15,27] and the analysis of the thermal decomposition of the foaming agent. It is known that, upon heating, $NaHCO_3$ decomposes endothermically producing carbon dioxide (g), water (g), and sodium carbonate (s). Since decomposition of $NaHCO_3$ and curing reactions must take place at the same time to obtain rigid foams, it is necessary to establish a processing temperature leading to a compromise between the kinetics of both processes. According to the thermal decomposition behavior of $NaHCO_3$ determined by thermogravimetric analysis (TGA; see Supporting Information) and considering the optimal curing temperature of the reactive mixture, an oven

DOI: 10.1021/acssuschemeng.5b00114
ACS Sustainable Chem. Eng. 2015, 3, 1406−1411

temperature of 140 °C was defined for the curing-foaming process.

Figure 2 shows the evolution of the temperature at the bulk of the sample as a function of the time for two reactive mixtures

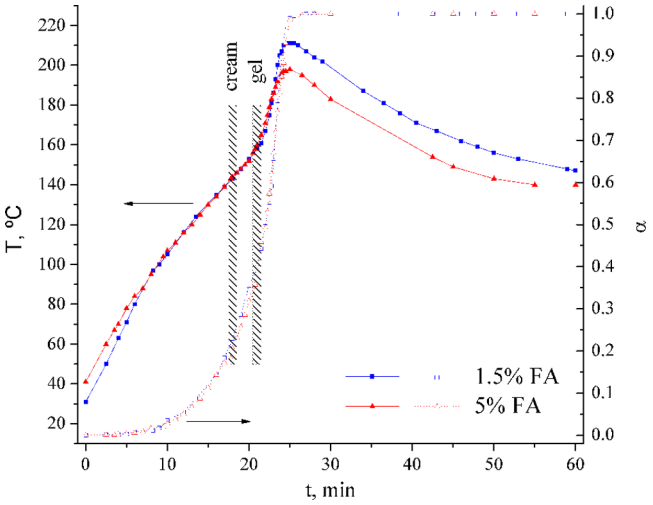

Figure 2. Temperature and conversion vs time profiles for two foaming systems, containing 1.5 (blue) and 5 wt % FA (red).

with different FA content, 1.5 and 5%. As expected, experimental cream and gel times (18 and 21 min, respectively) barely varied with FA content. Both samples attained the maximum temperature at about 27 min, but the formulation with the highest FA content exhibited the lowest temperature peak because a fraction of the heat released by the curing reaction was consumed by the thermal decomposition of $NaHCO_3$. According to the time−conversion curves, both formulations attained gelation at 50% conversion at similar gelation times. The completion of the reaction (100% conversion at 30 min) defined the processing window at the studied temperature.

Density and Morphology. Table 1 summarizes the apparent density (ρ^*), cell diameter (Dc), number of cells by surface area (n), and porosity (e) for the different formulations. All samples showed a slight variation of the local apparent density with the position as revealed by the dispersion of data. This behavior is usually found in polymeric foams, and it is due to different processes occurring simultaneously. In the first place, mold walls induce distinct bubble nucleation and growing processes in the parts of the foam growing close to them, leading to different morphologies compared with those that can be found in the central region.[1,28] Furthermore, drainage produced before gelation due to hydrostatic pressure gradient accounts for the apparent density increment from the top to the bottom of the foam.[1,28,29]

Table 1. Apparent Density (ρ^*), Cell Diameter (Dc), Cells by Surface Area (n), and Porosity (e) for Different FA Contents[a]

FA %	ρ^*, kg/m^3	Dc, μm	n, mm^{-2}	e
1	501 ± 49 a	680 ± 157 a	1.302	0.548
1.5	482 ± 45 a	490 ± 109 b	2.148	0.560
2.5	380 ± 70 b	483 ± 90 b	2.604	0.644
3.5	291 ± 64 c	572 ± 90 b	2.930	0.732
5	202 ± 41 d	518 ± 126 b	3.158	0.812
7	193 ± 35 d	534 ± 152 b	3.353	0.826

[a]Same letters in each individual column indicate that means difference is not significant in comparison by pairs (Tukey test with significance level α = 0.05).

No significant differences in average cell diameters were detected with increasing FA content, except for foams with 1% FA, which had slightly larger cells. Since cell concentration increases with FA content, it can be inferred that the higher amount of neighboring cells for FA > 1% leads to smaller cells compared with foams with 1% FA. The increasing cell concentration also accounts for the higher porosity (i.e., density decrease) as FA% increases, as revealed by the monotonous increment in both n and e values (Table 1).

Average apparent density values dropped from 500 to around 200 kg/m^3 when FA content was increased from 1% to 5% and remained nearly constant for higher FA contents. This density range is in line with those found for epoxy foams based on commercial synthetic systems[25,30] but is somewhat broader than those reported for other partially biobased epoxy foams.[18−21]

The cellular structure of ESO foams was studied by SEM, and some representative images taken from horizontal and vertical planes are shown in Figures 3 and 4, respectively. A

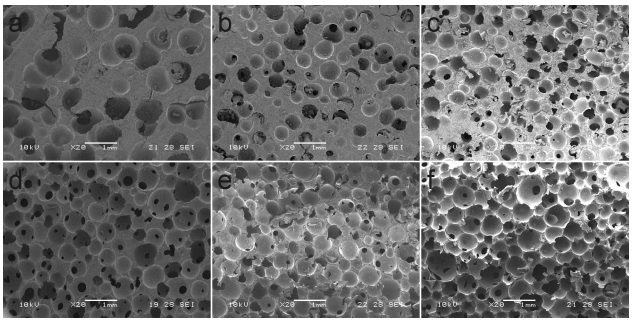

Figure 3. Horizontal plane SEM micrographs of foams with (a) 1% FA; (b) 1.5% FA; (c) 2.5% FA; (d) 3.5% FA; (e) 5% FA; (f) 7% FA.

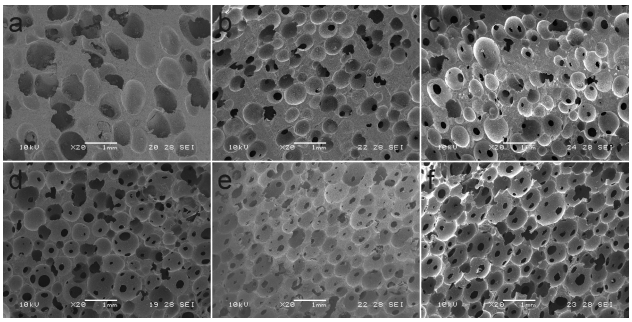

Figure 4. Vertical plane SEM micrographs of foams with (a) 1% FA; (b) 1.5% FA; (c) 2.5% FA; (d) 3.5% FA; (e) 5% FA; (f) 7% FA. Growth direction is vertical.

mixture of open and closed cells was evident in all foams regardless of either the FA content or the apparent density. In all cases, foam cells were uniformly distributed and the open-cells proportion seemed to increase at high FA contents. When the vertical plane was analyzed, deformed cells were noticed in the foam growth direction. This effect is usually observed when foam grows freely in one preferential direction, but it is constrained in the others by the mold in which the foaming

DOI: 10.1021/acssuschemeng.5b00114
ACS Sustainable Chem. Eng. 2015, 3, 1406−1411

process takes place.[31,32] When these restrictions are present, anisotropic stresses are generated in the whole volume and cells tend to grow preferentially in one direction, giving place to nonspherical bubbles.[32] Indeed, a slight deviation from the vertical direction was evidenced in some of the images of Figure 4, which was ascribed to the shape of the aluminum mold.

Mechanical Properties. Figure 5 shows some representative compressive stress (σ)-strain (ε) curves obtained in the

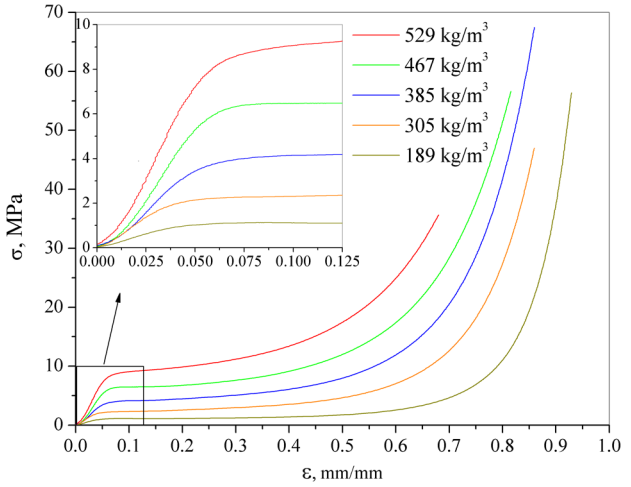

Figure 5. Compressive stress−strain curves obtained for foams with different densities.

foam growth direction, representing the typical behavior of thermosetting foams (compressive tests in the transversal direction with respect to the foam growth showed a similar shape; see Supporting Information). For ε values between 0.04 and 0.06, the foam exhibited the linear-elastic deformation (inset in Figure 5). After reaching the elastic limit, the collapse of the cells begins and the curves exhibited a sustained plateau followed by an increment with ε, due to the foam densification.

The value of strain at which densification starts (ε_D) is an important parameter, especially for foams used in shock absorption applications. Gibson and Ashby[33] gave a simple formula to estimate the ε_D for polymeric foams with relative densities between 0.2 and 0.4 (eq S3; Supporting Information). According to this, ε_D decreases with density, which seems to be in agreement with Figure 5.

However, Tan et al.[34] proposed a different approach based on the energy absorption efficiency, which led to different results, by giving similar ε_D values for all foams regardless of the density. In view of the analysis and comparison of both methods (see Supporting Information for further details), the results obtained by the last method gave a better representation of the foams' behavior, and therefore it can be stated that ε_D values for all of these foams are close to 0.5.

The pictures shown in Figure 6 provide a more detailed insight of the foams' behavior during compressive tests. A number of oblique lines were painted on one side of the specimen before testing, and from the deformation paths of those lines, some features of the compressive test can be inferred. The first images (a−g; $\varepsilon \approx 0-0.17$) showed a uniform deformation, with the lines maintaining essentially its shape and changing only its width and the angle with respect to the horizontal direction. In image h ($\varepsilon \approx 0.19$), a break in the lower part of the lines can be observed, indicating the collapse of a cell layer. Subsequently, several breaks were clearly evident, as a

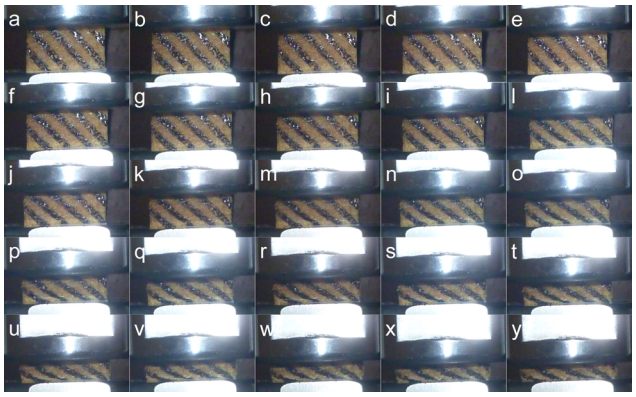

Figure 6. Sequence of pictures of a test sample (ρ = 385 kg/m^3) during a uniaxial compressive test.

result of the progressive collapse of cell layers at different heights. Finally (u−y; $\varepsilon \approx 0.5-0.7$), nearly straight lines were formed again when densification starts and compressive strain becomes uniform throughout the specimen height.

Compressive performance of rigid foams depends on their density, which is in turn related with the foaming agent content in each formulation. The compressive strength and compressive modulus of foams in the foam growth and in the transversal directions are summarized in Table 2. Compressive modulus and compressive strength decrease with increasing content of the blowing agent, which is consistent with the reduction in the apparent density. Compressive properties evaluated in the growth and transversal directions did not differ significantly for each formulation. It is clear from this that the slight anisotropy observed in the morphological study did not influence the compressive mechanical parameters.

It is noteworthy that, for similar densities, compressive strength is around 40% lower than those of partially biobased epoxy-amine foams,[21] but it is about 1.5 times higher than those reported for synthetic epoxy foams[25] and for AESO based foams,[18] and 1−3 orders of magnitude higher when compared to other nonreinforced biobased foams.[19,20,35,36]

Dynamic-Mechanic Thermal Analysis. Figure 7 shows the temperature dependence of the storage modulus and the damping factor of ESO-based foams. Foams with densities of 190 and 380 kg/m^3 (corresponding to 7% and 2% FA contents, respectively), and the nonfoamed ESO/MTHPA/1MI counterpart were analyzed. G' curves showed the typical shape of thermosetting polymers, with a high glassy modulus, and a sharp decrease in the glass transition region followed by a rubbery plateau characterized by an increase of G' with temperature, indicating the presence of permanent cross-linking points. It can be noted that G' decreased with density as expected according to the results shown in the Mechanical Properties section.

Besides the decrease of G' for the foams, the main difference between the three samples is the wider transition region registered for the solid nonfoamed formulation that could be also evidenced in the tan δ curves. Interestingly, the temperature at which G' dropped slightly varied with the addition of the FA and surfactant. The ESO/MTHPA/1MI matrix showed a tan δ peak temperature about 5 °C higher than that of the foams (70 ± 1 °C and 65 ± 1 °C, respectively). There are two plausible explanations for this finding. On one hand, the fatty acids used as a surfactant could act as a plasticizer, increasing the chain's mobility and reducing the tan

DOI: 10.1021/acssuschemeng.5b00114
ACS Sustainable Chem. Eng. 2015, 3, 1406−1411

Table 2. Compressive Modulus (E^*) and Compressive Strength (σ_c) in the Growth and Transversal Direction for the Different Foams[a]

	growth direction		transversal direction	
FA %	E^*, MPa	σ_c, MPa	E^*, MPa	σ_c, MPa
1	168.0 ± 49.5 a	8.17 ± 2.40 a	155.2 ± 38.8 a	7.90 ± 1.50 a
1.5	142.3 ± 39.4 a,b	6.82 ± 2.37 a	124.6 ± 27.6 a	6.55 ± 1.00 a
2.5	99.7 ± 42.2 b,c	4.60 ± 1.87 b	87.3 ± 20.5 b	4.26 ± 1.24 b
3.5	61.6 ± 28.3 c,d	2.83 ± 1.38 b,c	52.0 ± 13.2 c	2.50 ± 0.59 c
5	33.0 ± 19.1 d	1.53 ± 0.64 c	28.4 ± 5.63 d	1.04 ± 0.23 d
7	27.7 ± 15.6 d	1.21 ± 0.43 c	23.3 ± 5.6 d	1.05 ± 0.2 d

[a]Same letters in each individual column indicate that means difference is not significant in comparison by pairs (Tukey test with significance level α = 0.05).

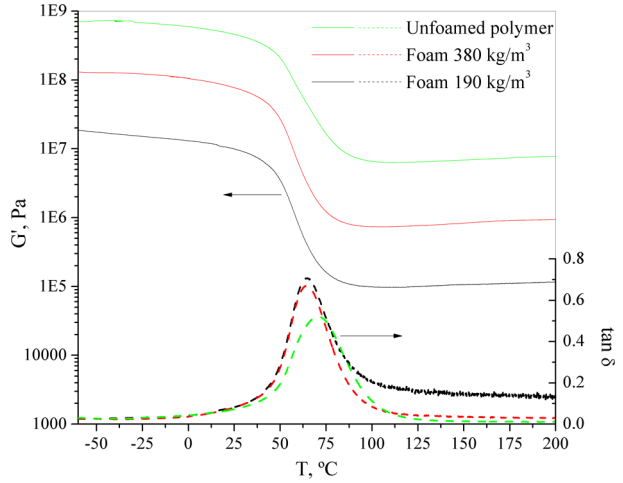

Figure 7. Storage modulus (G') and damping factor (tan δ) variation with temperature.

δ peak temperature. It can also be possible that water released by the thermal decomposition of the FA interferes with the chain polymerization reaction, lowering the cross-linking density. However, for many practical applications of these materials, this difference can be considered as not significant, and the tan δ peak values are not far from those found by Stefani et al. for commercial synthetic epoxy foams (up to 85 °C).[25]

CONCLUSIONS

Epoxy foams with a high biobased content were successfully synthesized and characterized. According to the results displayed in this paper, epoxidized vegetables oils constitute a suitable replacement for traditional epoxy resins based on fossil resources for the preparation of rigid polymeric foams. It was demonstrated, as well, that the use of highly toxic materials such as amines can be substantially reduced, and that epoxy foams can be produced using an innocuous (no ozone depleting, flammable, or toxic) foaming gas. The mechanical properties exhibited by these foams are the most relevant aspect of those described in the manuscript, being comparable with those exhibited by their fully synthetic counterpart. When compared with other partially biobased foams, it can be stated that the best compromise between mechanical properties, ease for preparation, and range of densities was achieved. Moreover, the potential of further broadening the density range by the application of processing techniques that are still under study should be mentioned. From the results obtained, we can ensure that these EVO based thermosetting foams constitute a valuable alternative to be used in similar applications to the commercial epoxy foams.

ASSOCIATED CONTENT

Supporting Information

Analysis of the thermal decomposition of the foaming agent. Kamal-Sourour kinetic equation and the ESO-MTHPA-1MI corresponding parameters. Compressive tests in the transversal direction. Compressive modulus (E^*) and compressive strength (σ_c) in the growth and transversal direction as a function of apparent density (ρ^*). Evaluation of the strain at which densification starts (ε_D). The Supporting Information is available free of charge on the ACS Publications website at DOI: 10.1021/acssuschemeng.5b00114.

AUTHOR INFORMATION

Corresponding Author

*Tel.: +54 223 481 6600 (183). Fax: +54 223 4810046. E-mail: faltuna@fi.mdp.edu.ar.

Funding

National Research Council (CONICET); National Agency of Scientific and Technological Promotion (ANPCyT); National University of Mar del Plata (UNMdP); Fundación Bunge y Born.

Notes

The authors declare no competing financial interest.

ACKNOWLEDGMENTS

The authors would like to thank the National Research Council (CONICET), the National Agency of Scientific and Technological Promotion (ANPCyT), and the National University of Mar del Plata (UNMdP) for the funding. F.I.A. also gratefully acknowledges the financial support from the Fundación Bunge y Born.

ABBREVIATIONS

OVCs, organic volatile compounds; Tg, glass transition temperature; EVOs, epoxidized vegetable oils; AESO, acrylated epoxidized soybean oil; MA, malonic acid; ESO, epoxidized soybean oil; DGEBA, diglycidyl ether of bisphenol A; MTHPA, methyltetrahydrophtalic; 1MI, 1-methyl imidazole; FA, foaming agent; t_{GEL}, gelation time; ρ^*, foam apparent densities; ϵ, porosity; ρ_s, polymeric matrix density; SEM, scanning electron microscopy; Dc, cell diameter; n, average number of cells by surface area; E^*, compressive apparent modulus; σ_c, compressive strength; G', storage shear modulus; tan δ, damping factor; ANOVA, analysis of variance; t_{cr}, cream time; σ, tension; ε, deformation; ε_D, densification strain

DOI: 10.1021/acssuschemeng.5b00114
ACS Sustainable Chem. Eng. 2015, 3, 1406−1411

REFERENCES

(1) Shutov, F. A.; Henrici-Olivé, G.; Olivé, S. *Integral/structural polymer foams: technology, properties, and applications*; Springer-Verlag: Berlin, 1985.

(2) Mondy, L. A.; Rao, R. R.; Moffat, H.; Adolf, D.; Celina, M. Structural Epoxy Foams. In *Epoxy polymers: new materials and innovations*; Wiley-VCH: Weinheim, 2010.

(3) Tschan, M. J.-L.; Brulé, E.; Haquette, P.; Thomas, C. M. Synthesis of biodegradable polymers from renewable resources. *Polym. Chem.* **2012**, *3* (4), 836−851.

(4) Corma, A.; Iborra, S.; Velty, A. Chemical Routes for the Transformation of Biomass into Chemicals. *Chem. Rev.* **2007**, *107* (6), 2411−2502.

(5) Chen, G.-Q.; Patel, M. K. Plastics Derived from Biological Sources: Present and Future: A Technical and Environmental Review. *Chem. Rev.* **2012**, *112* (4), 2082−2099.

(6) Yao, K.; Tang, C. Controlled Polymerization of Next-Generation Renewable Monomers and Beyond. *Macromolecules* **2013**, *46* (5), 1689−1712.

(7) Sun, X. S.; Wool, R. P. *Bio-based polymers and composites*; Elsevier, Acad. Press: Amsterdam, 2005.

(8) Gandini, A. The irruption of polymers from renewable resources on the scene of macromolecular science and technology. *Green Chem.* **2011**, *13* (5), 1061.

(9) Biermann, U.; Bornscheuer, U.; Meier, M. A. R.; Metzger, J. O.; Schäfer, H. J. Oils and Fats as Renewable Raw Materials in Chemistry. *Angew. Chem., Int. Ed.* **2011**, *50* (17), 3854−3871.

(10) Lligadas, G.; Ronda, J. C.; Galià, M.; Cádiz, V. Renewable polymeric materials from vegetable oils: a perspective. *Mater. Today* **2013**, *16* (9), 337−343.

(11) Miao, S.; Wang, P.; Su, Z.; Zhang, S. Vegetable-oil-based polymers as future polymeric biomaterials. *Acta Biomater.* **2014**, *10* (4), 1692−1704.

(12) Quirino, R. L.; Garrison, T. F.; Kessler, M. R. Matrices from vegetable oils, cashew nut shell liquid, and other relevant systems for biocomposite applications. *Green Chem.* **2014**, *16* (4), 1700.

(13) Boquillon, N.; Fringant, C. Polymer networks derived from curing of epoxidised linseed oil: influence of different catalysts and anhydride hardeners. *Polymer* **2000**, *41* (24), 8603−8613.

(14) Czub, P. Characterization of an Epoxy Resin Modified with Natural Oil-Based Reactive Diluents. *Macromol. Symp.* **2006**, *245*−*246* (1), 533−538.

(15) Altuna, F. I.; Espósito, L. H.; Ruseckaite, R. A.; Stefani, P. M. Thermal and mechanical properties of anhydride-cured epoxy resins with different contents of biobased epoxidized soybean oil. *J. Appl. Polym. Sci.* **2011**, *120* (2), 789−798.

(16) Auvergne, R.; Caillol, S.; David, G.; Boutevin, B.; Pascault, J.-P. Biobased Thermosetting Epoxy: Present and Future. *Chem. Rev.* **2014**, *114* (2), 1082−1115.

(17) Samper, M. D.; Petrucci, R.; Sánchez-Nacher, L.; Balart, R.; Kenny, J. M. New environmentally friendly composite laminates with epoxidized linseed oil (ELO) and slate fiber fabrics. *Compos. Part B Eng.* **2015**, *71*, 203−209.

(18) Bonnaillie, L. M.; Wool, R. P. Thermosetting foam with a high bio-based content from acrylated epoxidized soybean oil and carbon dioxide. *J. Appl. Polym. Sci.* **2007**, *105* (3), 1042−1052.

(19) Yadav, R.; Shabeer, A.; Sundararaman, S.; Chandrashekhara, K.; Flanigan, V.; Kapila, S. Development and Characterization of Soy-based Epoxy Foams. *Proceeding SAMPE Conf.* **2006**, 1−10.

(20) Doğan, E.; Küsefoğlu, S. Synthesis and *in situ* foaming of biodegradable malonic acid ESO polymers. *J. Appl. Polym. Sci.* **2008**, *110* (2), 1129−1135.

(21) Lau, T. H. M.; Wong, L. L. C.; Lee, K.-Y. Bismarck, A. Tailored for simplicity: creating high porosity, high performance bio-based macroporous polymers from foam templates. *Green Chem.* **2014**, *16* (4), 1931−1940.

(22) Altuna, F. I.; Espósito, L.; Ruseckaite, R. A.; Stefani, P. M. Syntactic foams from copolymers based on epoxidized soybean oil. *Compos. Part Appl. Sci. Manuf.* **2010**, *41* (9), 1238−1244.

(23) Altuna, F. I.; Piacentini, C. A. L.; Ruseckaite, R. A.; Stefani, P. M. Espumas Termorrígidas basadas en Aceites Vegetales Epoxidados (Thermosetting Foams based on Epoxidized Vegetable Oils). AR089614 A1.

(24) Altuna, F. I.; Pettarin, V.; Martin, L.; Retegi, A.; Mondragon, I.; Ruseckaite, R. A.; Stefani, P. M. Copolymers based on epoxidized soy bean oil and diglycidyl ether of bisphenol a: Relation between morphology and fracture behavior. *Polym. Eng. Sci.* **2014**, *54* (3), 569−578.

(25) Stefani, P. M.; Tejeira Barchi, A.; Sabugal, J.; Vazquez, A. Characterization of epoxy foams. *J. Appl. Polym. Sci.* **2003**, *90* (11), 2992−2996.

(26) Kamal, M. R.; Sourour, S. Kinetics and thermal characterization of thermoset cure. *Polym. Eng. Sci.* **1973**, *13* (1), 59−64.

(27) Altuna, F. I.; Riccardi, C. C.; Ruseckaite, R. A.; Stefani, P. M. Curado no-isotérmico de mezclas epoxi-aceite de soja epoxidado-anhídrido/Non-isothermal curing of epoxy-epoxidized soybean oil-anhydride mixtures. *Av. En Cienc. E Ing.* **2011**, *2* (4), 69−80.

(28) Exerowa, D.; Krugljakov, P. M.; Krugljakov, P. M.; Krugljakov, P. M. *Foam and foam films: theory, experiment, application*; Elsevier: Amsterdam, 1998.

(29) Adamson, A. W.; Gast, A. P. *Physical chemistry of surfaces*; Wiley: New York, 1997.

(30) Alonso, M. V.; Auad, M. L.; Nutt, S. Short-fiber-reinforced epoxy foams. *Compos. Part Appl. Sci. Manuf.* **2006**, *37* (11), 1952−1960.

(31) Eaves, D. *Handbook of polymer foams*; Rapra Technology: Shawbury, 2004.

(32) Klempner, D.; Sendijarevi'c, V.; Aseeva, R. M. *Handbook of polymeric foams and foam technology*; Hanser Publishers; Hanser Gardener [i.e. Gardner] Publications: Munich, 2004.

(33) Gibson, L. J.; Ashby, M. F. *Cellular solids: structure and properties*; Cambridge University Press: Cambridge, 1999.

(34) Tan, P. J.; Reid, S. R.; Harrigan, J. J.; Zou, Z.; Li, S. Dynamic compressive strength properties of aluminium foams. Part I—experimental data and observations. *J. Mech. Phys. Solids* **2005**, *53* (10), 2174−2205.

(35) Wang, H. J.; Rong, M. Z.; Zhang, M. Q.; Hu, J.; Chen, H. W.; Czigány, T. Biodegradable Foam Plastics Based on Castor Oil. *Biomacromolecules* **2008**, *9* (2), 615−623.

(36) Cornille, A.; Dworakowska, S.; Bogdal, D.; Boutevin, B.; Caillol, S. A new way of creating cellular polyurethane materials: NIPU foams. *Eur. Polym. J.* **2015**, *66*, 129−138.

DOI: 10.1021/acssuschemeng.5b00114
ACS Sustainable Chem. Eng. 2015, 3, 1406−1411